Patient-Specific Simulation of Implant Placement and Function for Cochlear Implantation Surgery Planning

Mario Ceresa[1], Nerea Mangado Lopez[1], Hector Dejea Velardo[1], Noemi Carranza Herrezuelo[3], Pavel Mistrik[4], Hans Martin Kjer[5], Sergio Vera[6], Rasmus R. Paulsen[5], and Miguel Angel González Ballester[1,2]

[1] Simbiosys group, Universitat Pompeu Fabra, Barcelona, Spain
[2] ICREA, Barcelona, Spain
[3] Multicellular system biology group, Centre for Genomic Regulation, Barcelona, Spain
[4] Med-EL, Innsbruck, Austria
[5] Denmark Technical University, Copenhagen, Denmark
[6] Alma IT Systems, Barcelona, Spain

Abstract. We present a framework for patient specific electrical stimulation of the cochlea, that allows to perform in-silico analysis of implant placement and function before surgery. A Statistical Shape Model (SSM) is created from high-resolution human μCT data to capture important anatomical details. A Finite Element Model (FEM) is built and adapted to the patient using the results of the SSM. Electrical simulations based on Maxwell's equations for the electromagnetic field are performed on this personalized model. The model includes implanted electrodes and nerve fibers. We present the results for the bipolar stimulation protocol and predict the voltage spread and the locations of nerve excitation.

1 Introduction

Hearing impairment or loss is among the most common reasons for disability. Worldwide, 27% of men and 24% of women above the age of 45 suffer from hearing loss of 26dB or more. The cochlear implant (CI) is a surgically placed device that converts sounds to electrical signals, bypassing the hair cells and directly stimulating the auditory nerve fibers.

Even if cochlear implantation is able to restore hearing in patients with severe or complete functional loss, the level of restoration varies highly between subjects and depends on a variety of patient-specific factors [1]. Moreover, extreme care has to be taken when inserting the CI's electrode array into the cochlea to obtain the best possible positioning while not damaging residual hearing capabilities [2].

The HEAR-EU[1] project aims at reducing the inter-patient variability in the outcomes of surgical electrode implantation by improving CI designs and surgical protocols. In this context, we propose that the availability of an accurate

[1] `http://www.hear-eu.eu/`

P. Golland et al. (Eds.): MICCAI 2014, Part II, LNCS 8674, pp. 49–56, 2014.

and personalized stimulation model of the cochlea can improve implant design, insertion planning and selection of the best treatment strategy for each patient.

In this work a model is built from high-resolution μCT data to create a detailed simulation of the electrical properties of the cochlea. To the best of our knowledge, this is the first study combining human high-resolution imaging techniques, finite element (FE) methods and a nerve fiber model to predict implantation results in humans. Previous works used synthetic geometrical models [3,4,5] or were restricted to animals [6]. In this work, we advance the state of the art by using a realistic and anatomically detailed model of the cochlea based on a statistical shape model (SSM) created using human μCT images.

Using our model, we can predict potential spread in the cochlea and location of nerve activation after surgery. As higher spreads correlate with inter-electrode interference and distorted pitch perception, we can use the results of our model to detect which configurations of electrode placement are to be avoided during surgery.

The rest of the paper is structured as follows: Section 2 describes the methodology for image acquisition and processing, the creation of the SSM, of the FEM mesh and its adaptation for specific patients. Section 3 describes the electrical conduction model and the different experiments performed. Section 4 presents the neural nerve fiber model and its initialization with the results of the FEM simulations. Results are reported in Section 5 and discussion and directions for future work are provided in Section 6.

2 FEM Construction and SSM-Based Patient-Specific Adaptation

Our model is based on 17 temporal bones excised from human cadavers. The samples were dried and scanned with a high-resolution Scanco μCT 100 system (Scanco Medical AG, Switzerland). Each dataset has a nominal isotropic resolution of 24.5 μm.

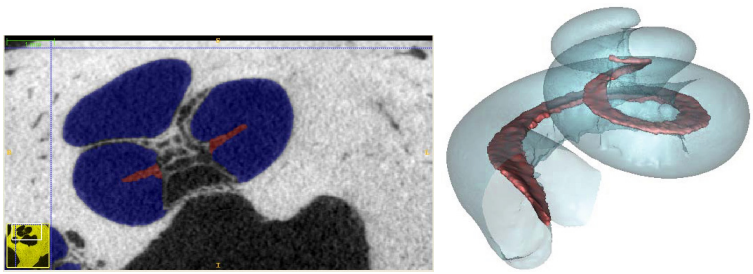

(a) (b)

Fig. 1. a) Segmented transversal slice of the μCT, showing the cochlea (blue) and the spiral bone (red). b) Surface reconstruction of the cochlea, built from the μCT image.

After acquisition, data was segmented using a semi-automatic level-set method [7] and manual corrections. Fig. 1a shows a transversal slice of the μCT image, where the cochlea is segmented in blue and the bony spiral lamina in red. Once segmented, the surface of the cochleas were extracted from the segmentation using Marching Cubes [8]. A Markov Random Field surface reconstruction was applied [9] to obtain a surface more suited for generating a FEM mesh. Fig. 1b shows a 3D surface reconstruction based on the μCT image.

In order to create the SSM one dataset was chosen as a reference and an initial rigid transformation aligning the center of mass and the principal directions was calculated. Then the transformations were applied to the reference surface model to create surfaces representing the anatomy in the individual datasets and a point distribution model (PDM) was built. Further information are available in [10]. The SSM can be instantiated to generate deformation fields corresponding to valid deformations of cochlear shapes, and in particular, it can be used to find the deformation that best fits the patient's image data.

The FEM mesh is built from the surface model with the exception of the basilar membrane and the nerves that are created manually (Figure 2). A sensitivity analysis to prove the accuracy versus computational cost of the model was carried out, leading to a finite element mesh of 8.764.7273 tetrahedral elements.

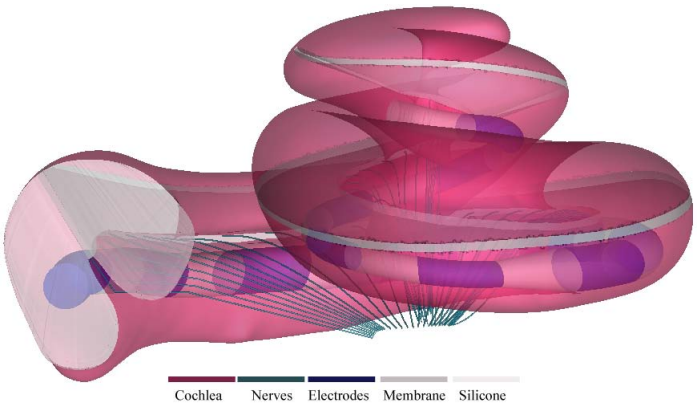

Fig. 2. Geometry of the FEM of the cochlea. Different colors represent the cochlea (purple), the nerves (aquamarine), the electrodes (violet), the basilar membrane (gray) and the silicon insulator (white). The maximum size of element selected for each part of the model and their electrical conductivity associated are as follows: 0.4, 0.005, 0.01, 0.008 , 0.8 (mm) and 1.43, 0.3, 1e7, 0.09375 and 1e-3 (S/m) for the cochlea, nerves, electrodes, membrane and silicone, respectively.

In our full pipeline the FE mesh is created on the mean shape of the SSM. This mesh is registered to the patient data, usually a lower resolution CT scan, in order to transfer the results to the clinical setting. The registration is regularized by the anatomical variability learnt in the shape model. This will produce a

geometrical fit but also capture the change in cochlear turning and basilar membrane length in an anatomical appropriate manner, thus making the simulation really patient specific.

The aspect ratio of FEM elements was checked in order to ensure a good mesh quality and the effect of the deformation on the quality of the elements is studied in [11]. All bio-mechanical properties and boundary conditions are also propagated, so new simulations can be run directly on the patient-specific mesh.

3 Electrical Conduction Model and Implant Stimulation Protocol

In order to simulate the electrical potentials we used the electrostatic solver of the open source tool Elmer [12]. We choose to use the quasi-static approximation and solve in this regime the Poisson equation:

$$\nabla \cdot \sigma \nabla \phi = \frac{\partial \rho}{\partial t} \tag{1}$$

where σ is the electric conductivity, ϕ the electric scalar potential and ρ the total charge density. For electric potential either Dirichlet or Neumann boundary condition can be used. The former prescribes the value of the potential on specified boundaries, the latter the current J_b on specified boundaries. Additional information on the electric model is available in [13]. A typical electrode array with 12 contacts (based on Med-EL Flex^{soft}design) was modeled and inserted in the FE model (Figure 2). The electrode array is placed through the round window into scala tympani along the lateral wall under the cochlea partition. In the full pipeline the post-operative electrode-array position would be estimated from a post-op CT scan. This is interesting as a surgical planning tool, as the surgeon can evaluate optimal electrode array design and position.

The boundary conditions for the electrode activation in the FE model are given by a stimulation pattern generation (SPG) and modeled after the manufacturer's indications. In this work we present the results relative to the bipolar (BP) stimulation protocol, where one electrode emits the current and the other is set to ground. In the following text, we refer to the bipolar stimulation as BPij where i is the source electrode and j the one set to ground. Typical stimulation currents for electrodes are in range of 0.3-1 mA and we set 1mA for all experiments. The conductivity parameters for the electrical simulation are taken from reference [6] from closely related animals.

4 Nerve Fiber Model

In order to describe the electrical properties of the nerve fibers, we use the Generalized Schwarz-Eikhof-Frijns (GSEF) model [14]. Each fiber is composed by a peripheral axon, a soma and a central axon. It has 16 compartments (Figure 3) where the voltages sampled from the FE model are applied to initialize the model, for a total of 64 coupled non-linear first-order differential equations per

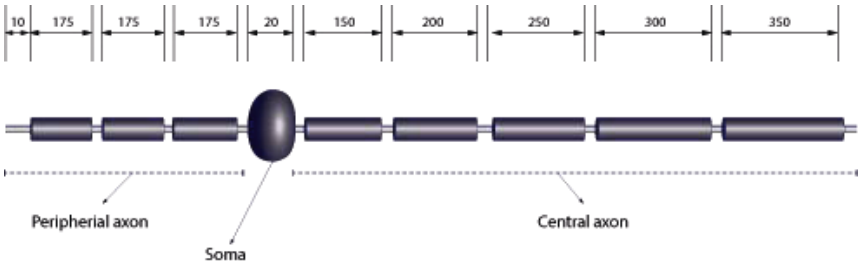

Fig. 3. Illustration of the first nodes of the nerve model used in our simulation, adapted from [14]. All dimensions are in μm, internodal gaps length is 1 μm, diameter of each compartment is 3 μm, except for the soma which is 10 μm. Internodal gaps represent the Ranvier nodes where we apply the voltage obtained by the FE model.

fiber. A total of 49 nervous fibers are modeled (Figure 2). In order to obtain the potential values to initialize our nerve model, we parameterized each of the 49 nerve bodies of the FEM using the arrival time from a heat diffusion equation. The parameterization was constructed in such a way that we could sample the potential field in 16 points per bodies, giving a total of 784 potential readings. Those points represent the un-myelinated parts of our fiber model, where the current flows in (Ranvier nodes). The readings in those points are shown in our potential spread plots (Figure 5). We implemented and solved the model in python using numpy, scipy and matplotlib open source tools [15].

5 Results

A total of 11 FE simulations were run in steady state formulation. Each simulation run until convergence on the cluster at our Institution, that consists of 11 compute nodes, with four 16-core processors per node, for a total of 704 cores and a peak of 7876 Gflops.

In Figure 4a we show an example simulation for the BP12 protocol, with the complete 3D model and electrode 1 setup as source and electrode 2 as ground. Solid lines represent the current flowing between the electrodes.

In Figure 4b we sampled the potentials from the BP12 stimulation in 784 points of the nerve mesh in order to feed them to the spiking model described in Section 4. The colors represent the intensity of the electric field. We see that the stimulation is stronger in the closest nerve, yet several other nerves are also affected.

In Figure 5 we present the readings of the electric field for each nerves under different stimulation protocols. On the horizontal axis we have the stimulation protocols and on the vertical axis the indexes of the nerves. Differences in electric reading depend on the size of the electrode and its distance from the recording nerve.

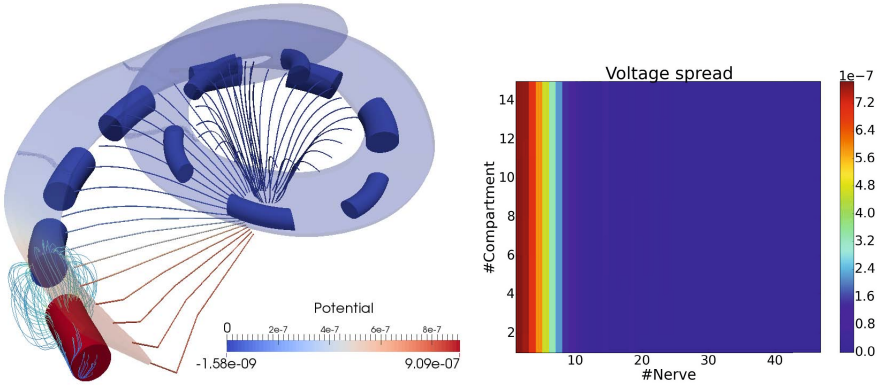

(a) (b)

Fig. 4. a) 3D view of BP12 stimulation protocol. Electrode 1 is active and emitting 1mA. Electrode 2 is set to ground. We can see how several nerves are affected by the stimulation. b) Voltage spread curve for BP12. Potential generated by the electrode is sampled in 49 nerves and 16 points per nerve for a total of 784 points. We see how the stimulation is not limited to the nerve closest to the electrode (nerve 1)

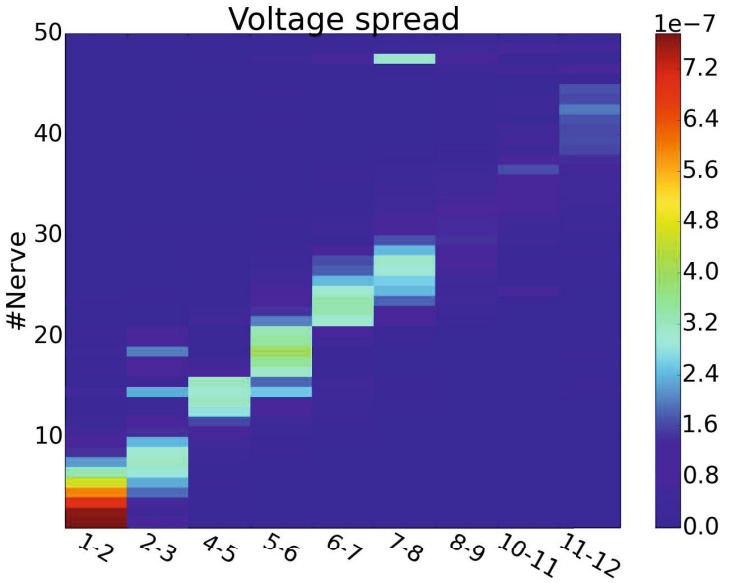

Fig. 5. Potential in each nerve for each stimulation protocol. We see how each electrode stimulates several nerves. Differences in potentials depend on the size of the electrode and its distance from the recording nerve.

In the presented results, we simulated electrode activation protocols BP1-2 to BP11-12 to show that we are able to deduce nerve activation and catch electrode cross-talk. Qualitatively, the modeled spread of excitation is in a reasonable agreement with clinical data published recently [16]. The predicted cross-talk between some of the most apical electrodes is in agreement with observations in some implanted patients [17].

The fact that, as can be seen from Figure 4b and 5, each electrodes activates more than one nerve, is at the basis of discrepancy between electrical and acoustical hearing perceptions. We thus plan to use the results of our model to predict which stimulation parameters and configurations of electrode placement are the best for each patient and thus improve the functional output of the CI surgery.

6 Discussion and Future Work

The main contribution of our work is the creation of a finite element (FE) model based on high-resolution human data and its use to predict nerve activation, which in turn allows the selection of the best electrode array for each patient from available electrode portfolios of established CI manufactures.

The model is tailored to humans and we believe that, once validated and refined, this model could be of great use for the optimization of the intracochlear position of an electrode array of an cochlear implant. We also believe it can be used for prediction of mapping in patients who cannot reliably provide auditory feedback such as, on one side, infants and young children, and on the other side, psychologically challenged patients.

This work is a step forward towards a complete personalization of CI surgery where array insertion strategy and expected response could be planned well ahead of the surgery. Virtual testing of new implants will in the future help surgeons to select the most suitable electrode array for an implant accordingly to the anatomy of the patient's cochlea. Further, being able to study the whole range of cochlear shapes and frequency distribution of the target population will lead to better fitting of implants, as well as a considerable cost reduction in the design process.

In order to assess the appropriateness of implant's electrode array design, further development should be done to define the different scenarios of the electrode array insertion, in terms of positions where it is likely to be placed and the percentage of residual hearing preserved.

Channel interaction predicted by the model will be evaluated in a follow up clinical study together with the correlation between cochlear anatomy, determined by pre-clinical CT scanning, and the spread of excitation. This will improve the selection of the best electrode array for each patient, with optimally distanced electrodes to minimize the cross-talk, from electrode portfolios available for CI surgery.

Acknowledgement. The research leading to these results received funding from the European Union Seventh Frame Programme (FP7/2007-2013) under grant agreement 304857.

References

1. World Health Organization: Deafness and hearing impairment (2012)
2. World Health Organization: The global burden of disease: 2004 update (2008)
3. Edom, E., Obrist, D., Kleiser, L.: Simulation of fluid flow and basilar-membrane motion in a two-dimensional box model of the cochlea. In: AIP Conference Proceedings, vol. 1403, p. 608 (2011)
4. Nogueira, W.: Finite element study on chochlear implant electrical activity. In: ICBT Proceeding (2013)
5. Nogueira, W., Penninger, R., Buchner, A.: A model of the electrically stimulated cochlea. In: DAGA Proceeding (2014)
6. Malherbe, T.K., Hanekom, T., Hanekom, J.J.: Can subject-specific single-fibre electrically evoked auditory brainstem response data be predicted from a model? Medical Engineering & Physics 35(7), 926–936 (2013)
7. Yushkevich, P.A., Piven, J., Hazlett, H.C., Smith, R.G., Ho, S., Gee, J.C., Gerig, G.: User-guided 3d active contour segmentation of anatomical structures: significantly improved efficiency and reliability. Neuroimage 31(3), 1116–1128 (2006)
8. Lorensen, W.E., Cline, H.E.: Marching cubes: A high resolution 3d surface construction algorithm. In: ACM Siggraph Computer Graphics, vol. 21, pp. 163–169 (1987)
9. Paulsen, R.R., Baerentzen, J.A., Larsen, R.: Markov random field surface reconstruction. IEEE Transactions on Visualization and Computer Graphics 16(4), 636–646 (2010)
10. Kjer, H., Vera, S., Perez, F., Gonzalez-Ballester, M., Paulsen, R.: Shape modeling of the inner ear from micro-ct data. In: Proceedings of Shape Symposium on Statistical Shape Models and Applications (2014)
11. Kjer, H.M., Ceresa, M., Carranza, N., Vera, S., Gonzalez-Ballester, M.A., Paulsen, R.R.: Cochlear finite element modelling, mesh quality under ssm-driven deformations. In: MeshMED Workshop - Medical Image Computing and Computer-Assisted Intervention, MICCAI 2013, pp. 70–78. Springer, Heidelberg (2013)
12. Ruokolainen, J., Lyly, M.: ELMER, a computational tool for PDEs–Application to vibroacoustics. CSC News 12(4), 30–32 (2000)
13. Råback, P., Malinen, M., Ruokolainen, J., Pursula, A., Zwinger, T.: Elmer models manual. CSC–IT Center for Science, Helsinki, Finland (2013)
14. Frijns, J.H.M., De Snoo, S., Schoonhoven, R.: Potential distributions and neural excitation patterns in a rotationally symmetric model of the electrically stimulated cochlea. Hearing Research 87(1), 170–186 (1995)
15. Oliphant, T.E.: Python for scientific computing. Computing in Science & Engineering 9(3), 10–20 (2007)
16. Vanpoucke, F.J., Boermans, P., Frijns, J.H.: Assessing the placement of a cochlear electrode array by multidimensional scaling. IEEE Transactions on Biomedical Engineering 59(2), 307–310 (2012)
17. Gani, M., Valentini, G., Sigrist, A., Kós, M.I., Boëx, C.: Implications of deep electrode insertion on cochlear implant fitting. Journal of the Association for Research in Otolaryngology 8(1), 69–83 (2007)